Collisions between spatiotemporal solitons of different dimensionality in a planar waveguide

Hector E. Nistazakis,[1] Dimitri J. Frantzeskakis,[1,*] and Boris A. Malomed[2]
[1]*Department of Physics, University of Athens, Panepistimiopolis, 157 84 Athens, Greece*
[2]*Department of Interdisciplinary Studies, Faculty of Engineering, Tel Aviv University, Tel Aviv 69978, Israel*
(Received 22 December 2000; revised manuscript received 12 March 2001; published 17 July 2001)

A $(2+1)$-dimensional nonlinear Schrödinger equation including third-order dispersion is a natural model of a waveguide, in which strong temporal dispersion is induced by a grating in order to make the existence of two-dimensional spatiotemporal solitons possible. By means of analytical and numerical methods, we demonstrate that this model may support, simultaneously, stable dark quasi-one-dimensional (stripe) solitons and two-dimensional elevation solitons (''antidark solitons'') in the form of weakly localized ''lumps.'' The spatial position of lumps can be controlled by passing stripe dark solitons through them in an arbitrary direction. To substantiate this mechanism, we analytically calculate a position shift generated by a headon collision between the stripe and lump. The obtained results are in good agreement with direct numerical simulations.

DOI: 10.1103/PhysRevE.64.026604 PACS number(s): 42.81.Dp, 42.65.Tg, 42.65.−k

I. INTRODUCTION

Recently, much attention in nonlinear optics has been attracted to *spatiotemporal* solitons (alias light bullets, LBs [1]), i.e., two- or three-dimensional (2D or 3D) objects localized in both space and time. Solitons of this type were first considered in models of saturable nonlinear media [2]. Then, they have been studied in second-harmonic-generating (SHG) media [3–7], in self-induced transparency [8,9], and, beyond the framework of nonlinear optics, in various models describing fluid flows [10]. Additionally, stable LBs of the ''antidark'' type, i.e., elevation solitons built up on top of a continuous-wave (cw) background, were predicted in a nonlinear Schrödinger (NLS) model [11], suggesting the possibility of the experimental observation of LBs of the latter type in a usual glass waveguide.

In a real experiment, spatiotemporal solitons in (effectively) two spatial dimensions have been thus far observed in waveguides with the SHG nonlinearity [7]. A typical size of the waveguide (monocrystal of a cubic shape) is ~ 3 cm, the temporal width τ of the soliton being less than 100 fs [7]. Obviously, the main difficulty in creation of well-formed spatiotemporal (or simply temporal [12]) solitons in so small samples is the lack of strong temporal dispersion, necessary to induce the soliton's dispersion length smaller than 1 cm. In the present work, we consider spatiotemporal solitons existing on top of a finite-amplitude cw background in a 2D medium with the ordinary Kerr nonlinearity, which corresponds to a usual planar glass waveguide. Nevertheless, practically possible experiments with solitons (thus far, these were spatial solitons) in glass waveguides are also limited to samples whose size is measured in centimeters [13], which broaches the same problem of creating very strong effective temporal dispersion in the waveguide.

A principal solution to the problem implemented in experiments [7,12] (and still earlier proposed theoretically [6]), is the creation of an artificial dispersion by means of a properly placed grating. However, it is commonly known that the grating induces not just the second-order temporal dispersion, which is postulated in the usual models of the spatiotemporal propagation, but its own dispersion law with a gap, which also gives rise to higher-order dispersions; first of all the third-order dispersion (TOD) (see, e.g., [14] for a review and a recent experimental work [15] specially focused on TOD induced by gratings). A straightforward estimate, based on this dispersion law and assuming the temporal width of the pulse ~ 100 fs, grating-induced reflection length ~ 1 mm, and dispersion length induced by the second-order dispersion ~ 1 cm, shows that, in fact, the corresponding TOD length is also ~ 1 cm. Therefore, taking into account the higher-order dispersion in models of spatiotemporal solitons may be quite important. In the present work, we make a step in this direction adding the TOD term to the model equation. It will be demonstrated that this modification results in qualitatively new results, opening a way to coexistence of solitons of different dimensions, viz., quasi-1D dark solitons and truly 2D elevation (''antidark'') solitons in the form of lumps.

In this connection, it is necessary to say that recent experiments have already initiated the study of interactions between *spatial* solitons of different dimensionality, namely, 1D and 2D ones. In particular, a collision of a 2D *bright* ''needle'' soliton with a 1D *bright* soliton stripe was observed in a photorefractive crystal [16], while interaction of a 1D *dark* soliton stripe with a 2D *dark* vortex soliton was studied in the rubidium vapor [17]. However, interactions of *spatio-temporal* solitons having different dimensionalities, for instance, a 1D stripe and a 2D lump, and/or different polarities, e.g., dark and ''antidark'' solitons, have not been addressed yet. It is among the purposes of this work to study these types of the interactions theoretically in a model of the nonlinear waveguide with the usual Kerr nonlinearity taking into regard TOD, which is necessary to describe a realistic situation, as it was explained above.

The consideration of an interaction between the dark stripes and ''antidark'' lumps is not merely a subject of theoretical interest. Indeed, passing a dark stripe soliton or, more generally, an array of stripes through a lump (if neces-

*Corresponding author. FAX: +301-725 7658. Email address: dfrantz@cc.uoa.gr

sary, the stripes may be launched in different directions) is a unique opportunity to *move* the lump in a controllable way (provided that the interaction-induced shift of the lump's position is calculated in advance, which we do in this work). Thus, the problem to be considered here directly suggests new experiments, which are quite feasible by means of available techniques [7]. In principle, a method that makes it possible to manipulate positions of 2D solitons in the waveguide may have implications for the design of optical data-processing systems, but it would be premature to discuss this application in detail here.

Getting back to the theoretical purport of the interaction problem, it is relevant to mention the well-known fact that collisions between lumps in equations of the *Kadomtsev-Petviashvili* (KP) type, to which the present model may be reduced (see below), yield shifts exactly equal to zero [18]. Therefore, a finite collision-induced position shift for a lump is, by itself, a nontrivial result.

For the analytical consideration of the problem, we employ a variation of the so-called Poincaré-Lighthill-Kuo perturbation method (see, e.g., [19]) to show that the solitons with different dimensionality (1D and 2D) and different polarity (dark and antidark) indeed coexist and, therefore, they may interact. We show that the corresponding field may be regarded as a superposition of two waves moving in opposite directions, which obey two different KP equations in the respective reference frames. One turns out to be the so-called KP-II equation, which has stable quasi-1D soliton solutions (corresponding to the 1D dark stripe), and the other is the KP-I equation, which gives rise to stable *lump* solutions of the elevation (antidark) type (while its quasi-1D solutions are unstable). A noteworthy feature of these lumps is that they are weakly (nonexponentially) localized, unlike 2D solitons of the usual (exponentially localized) type dealt with in Refs. [16], [17].

Having found these solutions in an analytical form, we then analytically calculate their position shifts induced by head-on collisions. The fact that the dark stripe and antidark LB undergo nearly elastic collisions, resembling collisions between genuine solitons in completely integrable systems, is confirmed by direct numerical simulations reported in this work too. Numerically computed solitons' collision-induced position shifts are found to be in a reasonable agreement (the largest discrepancy being 20%) with the analytical values predicted by the asymptotic approach.

II. THE MODEL AND ITS ANALYTICAL CONSIDERATION

The model equation, namely the $(2+1)$-dimensional NLS equation with the focusing Kerr nonlinearity, second-order dispersion (SOD), and TOD can be derived directly from the Maxwell's equations, applying to them the slowly-varying-envelope and paraxial approximations, and has a known normalized form [11],

$$iu_z+\tfrac{1}{2}\,(u_{xx}-\alpha u_{tt})+|u|^2u=i\beta u_{ttt} \tag{1}$$

(the derivation is straightforward too if the dispersion is induced by the above-mentioned grating, see Ref. [6]). In Eq. (1), $u(z,x,t)$ is a complex envelope of the electromagnetic field, which evolves along the longitudinal coordinate z, depending also on the transverse coordinate x and time t, while the constant parameters α and β are the SOD and TOD coefficients, respectively. Below, we assume that both α and β are positive, $\alpha>0$ corresponding to the normal dispersion.

Substituting $u=u_0\rho^{1/2}\exp(i\varphi)$ into Eq. (1), we derive the following system of equations:

$$\begin{aligned}\varphi_z-|u_0|^2\rho+\tfrac{1}{2}\,(\varphi_x^2-\alpha\varphi_t^2)-\tfrac{1}{2}\,\rho^{-1/2}[(\rho^{1/2})_{xx}-\alpha(\rho^{1/2})_{tt}]\\ -\beta\varphi_m-\beta\varphi_t^3-3\beta\rho^{-1/2}[\varphi_t(\rho^{1/2})_t]_t=0,\end{aligned} \tag{2}$$

$$\rho_z+(\rho\varphi_x)_x-\alpha(\rho\varphi_t)_t-\beta\rho_m+\tfrac{3}{4}\,\beta(\rho^{-1}\rho_t^2)_t+3\beta(\rho\varphi_t^2)_t=0. \tag{3}$$

Below, we intend to consider a configuration with two solitons A and B which initially (i.e., at $z=0$) are far apart from each other, moving in opposite directions with velocities $C^{(A)}$ and $C^{(B)}$ in the t-z plane, so that they are going to collide. Assuming small-amplitude solitons with amplitudes $\sim\varepsilon$, where $\varepsilon\ll 1$ is a formal perturbation parameter, we expect that the collision will be quasi-elastic, so as to cause only shifts of the postcollision soliton trajectories.

Fixing that the soliton $A(B)$ is moving to the right (left) in the t-z plane, we introduce stretched coordinates ξ and η, which are linked to the solitons and defined as follows:

$$\xi=\varepsilon^{1/2}(t-C^{(A)}z)+\varepsilon\xi_1(\eta,X,Z)+\varepsilon^{3/2}\xi_2(\eta,X,Z)+\cdots, \tag{4}$$

$$\eta=\varepsilon^{1/2}(t+C^{(B)}z)+\varepsilon\,\eta_1(\xi,X,Z)+\varepsilon^{3/2}\eta_2(\xi,X,Z)+\cdots, \tag{5}$$

$$X=\varepsilon x,\quad Z=\varepsilon^{3/2}z, \tag{6}$$

where ξ_j and η_j $(j=1,2,...)$ are coordinate perturbations describing collision effects, which will be found below by means of the perturbation method. The solitons' velocities $C^{(A)}$ and $C^{(B)}$ appearing in the definitions (4) and (5) are not arbitrary. The subsequent consideration will demonstrate that in the lowest approximation, they are determined by the amplitude of the cw background and higher-order corrections to them depend on characteristics of the solitons (amplitude, wave numbers, etc).

Equations (2) and (3) have a simple solution $\rho=1$ and $\varphi=|u_0|^2z$, where u_0 is an arbitrary complex constant, which corresponds to the cw solution to Eq. (1). Although this cw solution is subject to modulational instability in the case under consideration (the focusing Kerr nonlinearity and normal SOD), one can easily find conditions under which the instability band is effectively suppressed by a finite size of the waveguide [11]; it is also relevant to stress that newly developed experimental techniques indeed make it possible to observe 2D solitons (namely, vortices in SHG media) supported by a background that is formally subject to the modulational instability [20]. Thus, we expect that if the two solitons A and B were created on top of this cw background, their head-on collision will take place within an interval of the propagation distance z, which is much shorter than that necessary for onset of the modulational instability. As we will show below by direct numerical simulations, this is indeed the case.

We seek small-amplitude solutions to Eqs. (2) and (3) that propagate on top of the cw solution, which makes it natural to introduce the following expansions for the fields ρ and φ:

$$\rho = 1 + \varepsilon\rho_1 + \varepsilon^2\rho_2 + \cdots, \quad \varphi = |u_0|^2 z + \varepsilon^{1/2}\varphi_1 + \varepsilon^{3/2}\varphi_2 + \cdots, \tag{7}$$

where ρ_j and $\varphi_j\,(j=1,2,...)$ are functions of the stretched coordinates defined in Eqs. (4)–(6). Finally, assuming that, to the leading order in ε, the absolute values $C^{(A)}$ and $C^{(B)}$ of the soliton velocities [see Eqs. (4) and (5)] are equal, we introduce the following expansions for $C^{(A)}$ and $C^{(B)}$:

$$\begin{aligned} C^{(A)} &= C_0 + \varepsilon C_1^{(A)} + \varepsilon^2 C_2^{(A)} + \cdots, \\ C^{(B)} &= C_0 + \varepsilon C_1^{(B)} + \varepsilon^2 C_2^{(B)} + \cdots, \end{aligned} \tag{8}$$

where C_0 and $C_j^{(A)}, C_j^{(B)}\,(j=1,2,...)$ will be found below in terms of solitons' characteristics (amplitudes, wave numbers, etc).

Substituting Eqs. (4)–(8) into Eqs. (2) and (3), we obtain a hierarchy of coupled equations for the functions ρ_j and φ_j. To the leading order, i.e., to orders $O(\varepsilon)$ and $O(\varepsilon^{3/2})$, respectively, Eqs. (2) and (3) amount to two linear equations, whose solution has the following form. The amplitude perturbation ρ_1 is

$$\rho_1 = f_1(\xi,X,Z) + g_1(\eta,X,Z), \tag{9}$$

where the unknown functions $f_1(\xi,X,Z)$ and $g_1(\eta,X,Z)$ are to be determined at the next order. The phase perturbation φ_1 can be expressed in terms of the same functions,

$$\varphi_1 = -\frac{C_0}{\alpha}\int_{+\infty}^{\xi} f_1(\xi',X,Z)\,d\xi' + \frac{C_0}{\alpha}\int_{-\infty}^{\eta} g_1(\eta',X,Z)\,d\eta', \tag{10}$$

where the lower limits of the integration in Eq. (10) were chosen so as to make the initial phases of the two waves equal to zero. Finally, it is found that the unknown lowest-order velocity C_0 is determined by the equation

$$C_0^2 - \alpha|u_0|^2 = 0. \tag{11}$$

Thus, at the leading order, we have shown that the field is a superposition of two waves A and B described, respectively, by the functions $f_1(\xi,X,Z)$ and $g_1(\eta,X,Z)$, which are traveling with the same absolute value of the velocity in opposite directions in the t-z plane. The form of these functions will be derived below in the next-order approximation.

Proceeding to the next order, viz., $O(\varepsilon^2)$ and $O(\varepsilon^{5/2})$, Eqs. (2) and (3) give rise to the following results. First, we obtain expressions for the amplitude and phase functions ρ_2 and φ_2,

$$\rho_2 = f_2(\xi,X,Z) + g_2(\eta,X,Z), \tag{12}$$

$$\varphi_2 = -\frac{C_0}{\alpha}\int_{+\infty}^{\xi} f_2(\xi',X,Z)\,d\xi' + \frac{C_0}{\alpha}\int_{-\infty}^{\eta} g_2(\eta',X,Z)\,d\eta', \tag{13}$$

and the result (11) is obtained once again. As it is seen, these results are similar to those obtained in the leading-order approximation. The functions $f_2(\xi,X,Z)$ and $g_2(\eta,X,Z)$ can be found in the subsequent approximation, but they are not relevant for the present work.

Second, we obtain the following equations for the unknown amplitude-perturbation functions f_1 and g_1,

$$\left[f_{1Z} - C_1^{(A)} f_{1\xi} + \frac{3C_0}{2}\left(1 + \frac{2\beta C_0}{\alpha^2}\right) f_1 f_{1\xi} - \frac{\alpha^2}{8C_0} \times \left(1 + \frac{8\beta C_0}{\alpha^2}\right) f_{1\xi\xi\xi}\right]_{\xi} - \frac{C_0}{2\alpha} f_{1XX} = 0, \tag{14}$$

$$\left[g_{1Z} + C_1^{(B)} g_{1\eta} - \frac{3C_0}{2}\left(1 - \frac{2\beta C_0}{\alpha^2}\right) g_1 g_{1\eta} + \frac{\alpha^2}{8C_0} \times \left(1 - \frac{8\beta C_0}{\alpha^2}\right) g_{1\eta\eta\eta}\right]_{\eta} + \frac{C_0}{2\alpha} g_{1XX} = 0. \tag{15}$$

Both Eqs. (14) and (15) have the form of the KP equation in the reference frames (Z,ξ,X) and (Z,η,X), respectively. As we will see below, under certain conditions, Eqs. (14) and (15) possess stable soliton solutions of different dimensionality and polarity, namely, 1D dark and 2D elevation (antidark) solitons, respectively.

Finally, eliminating secular terms at the present order of the asymptotic approximation, we derive equations for the phase-perturbation functions ξ_1 and η_1,

$$\xi_{1\eta} = \frac{1}{4}\left(1 + \frac{6\beta C_0}{\alpha^2}\right) g_1, \tag{16}$$

$$\eta_{1\xi} = \frac{1}{4}\left(1 - \frac{6\beta C_0}{\alpha^2}\right) f_1. \tag{17}$$

In the next section, we will obtain soliton solutions to Eqs. (14) and (15) and then, making use of Eqs. (16) and (17), position shifts of solitons induced by their headon collision will be found.

III. ONE-DIMENSIONAL DARK AND TWO-DIMENSIONAL ELEVATION SOLITONS AND THEIR COLLISIONS

We now return to the KP equations (14) and (15) and assume, without loss of generality, that the leading-order soliton velocity C_0 is positive, i.e., $C_0=\alpha^{1/2}|u_0|$ as per Eq. (11). Then, it is easy to verify that Eq. (14) is a KP-II equation (i.e., the one with negative effective dispersion), while Eq. (15) is either a KP-II or a KP-I equation (i.e., it may have positive dispersion) depending on the value of the parameter,

$$\delta\equiv\alpha^{3/2}/\beta|u_0|. \tag{18}$$

In particular, if $\delta<2$ or $\delta>8$, Eq. (15) is KP-II, while if $2<\delta<8$, Eq. (15) is KP-I. Note that if $C_0=-\alpha^{1/2}|u_0|<0$, then the types of Eqs. (14) and (15) are reversed, i.e., the former one is either a KP-I or a KP-II equation, depending on the value of δ, and the latter equation is always KP-II, which means that the types of their soliton solutions (to be presented below) will change accordingly.

As is known [18], these two versions (KP-II and KP-I) of the KP equation give rise to soliton solutions of different types. Particularly, both the KP-II and KP-I equations have *stripe* (quasi-1D) soliton solutions, which are, respectively, stable and unstable in these two cases, and the KP-I equation additionally has stable *lump* (2D) soliton solutions. In our case, the stripe-soliton solution to Eq. (14) (i.e., the leading-order part of the soliton A) has the form

$$f_1(\xi,X,Z)=-\frac{\alpha\kappa_1^2}{|u_0|^2}\left(\frac{\delta+8}{\delta+2}\right)\mathrm{sech}^2[\kappa_1(\xi+\kappa_2X+\kappa_3Z)], \tag{19}$$

where the relation (11) was used, $\kappa_1,\kappa_2,\kappa_3$ are arbitrary constants characterizing the soliton's amplitude and wave numbers, and the positive parameter δ was defined above by Eq. (18). In this case, the first-order correction $C_1^{(A)}$ to the soliton's velocity is

$$C_1^{(A)}=-\frac{1}{2}\beta(\delta+8)\kappa_1^2-\frac{1}{2}\frac{\alpha\kappa_2^2}{\beta\delta}+\kappa_3. \tag{20}$$

Notice that in the case $\delta<2$ or $\delta>8$, Eq. (15), which describes the leading-order part of the soliton B, has a similar solution, i.e., a stable stripe soliton, which is not relevant for the present analysis. Importantly, the amplitude of the stripe soliton (19) is always negative, i.e., the soliton has the form of a dip on the cw background and as result this soliton is of the *dark* type.

We now proceed to the KP-I version of Eq. (15), assuming that $2<\delta<8$. In this case, the stripe (quasi-1D) soliton solution is unstable but there exist stable 2D solitons alias *lumps* [18]. In our case, the lump-soliton solution to Eq. (15) is

$$g_1(\eta,X,Z)=-\frac{2\alpha}{|u_0|^2}\left(\frac{\delta-8}{\delta-2}\right)\left\{\frac{-y^2+\lambda_1s^2+\lambda_1^{-1}}{[y^2+\lambda_1s^2+\lambda_1^{-1}]^2}\right\}, \tag{21}$$

$$y=\eta+\lambda_2Z, \tag{22}$$

$$s=\alpha|u_0|^{-1}[3\delta(8-\delta)]^{1/2}X, \tag{23}$$

where λ_1 and λ_2 are arbitrary constants. In this case, the first-order correction $C_1^{(B)}$ to the lump's velocity can also be found,

$$C_1^{(B)}=-\frac{3\lambda_1a^2\delta(\delta-8)}{8C_0}-\lambda_2. \tag{24}$$

The solution (21) is a 2D spatiotemporal soliton, which decays *algebraically* (slower than an exponential) as $(\eta^2+X^2)^{1/2}\rightarrow\infty$. As in this case the factor $(\delta-8)/(\delta-2)$ in the lump's amplitude must be negative, the solution (21) represents an antidark elevation on top of the cw background.

Thus, in the region $2<\delta<8$ the field obeying Eq. (1) is a superposition of two solitons, which move in opposite directions and have opposite polarities (dip/elevation) and different dimensionalities: a quasi-1D dark stripe (soliton A) and a 2D lump (soliton B), described by Eqs. (19) and (21), respectively. A nontrivial feature of this situation is a possibility of a headon collision between the two solitons, which is considered below. Note that this nontrivial situation may only occur in the presence of TOD. Indeed, if $\beta=0$, both Eqs. (14) and (15) turn out to be of the KP-II type, possessing solely dark stripe-soliton solutions.

The theoretical predictions, i.e., the coexistence and possibility of the headon collision of the small-amplitude quasi-1D (Q1D) dark line soliton and 2D elevation lump, have been verified by direct numerical integration of the underlying NLS equation (1). The analytical expressions given by Eqs. (19) and (21) were used as initial configurations at $z=0$ on top of a cw background of a finite extent. An actual shape of the background was a super-Gaussian $\exp(-[(x^2+t^2)/L^2]^8)$ (which is a realistic shape of a cylindrical optical beam created by laser systems). In the simulations, we have used the values $\alpha=0.1$ and $\beta=0.013$ for the SOD and TOD coefficients, respectively (which corresponds, in accordance with what was said in the Introduction, to relatively strong TOD). As for the solitons' parameters, we used $u_0=1$ for the cw background (and $L=90$ for the super-Gaussian), $\kappa_1=1.6$, $\kappa_2=0.2$ for the Q1D dark soliton, and $\lambda_1=0.8$, $\lambda_2=0.9$ for the 2D elevation lump, respectively, while the perturbation parameter was chosen to be $\varepsilon=0.25$.

Starting from the initial configuration shown in Fig. 1(a), different stages of the simulated headon collision are shown in Figs. 1(b)–1(e) for $z=7.5$, 13.5, 15, and 30, respectively. Additional details are shown by inset contour plots in each panel. As it is seen, although a small amount of radiation is emitted by both solitons, and deformation in their shapes is tangible (especially for the 2D lump), the collision is quasi-elastic: after passing through each other, the solitons basically restore their shapes. This behavior is in agreement with the analytical results of the perturbation theory developed above, which predicts that the headon collision is elastic up to the second order, but it becomes inelastic if higher-order corrections are included (i.e., the above corrections ρ_2 and

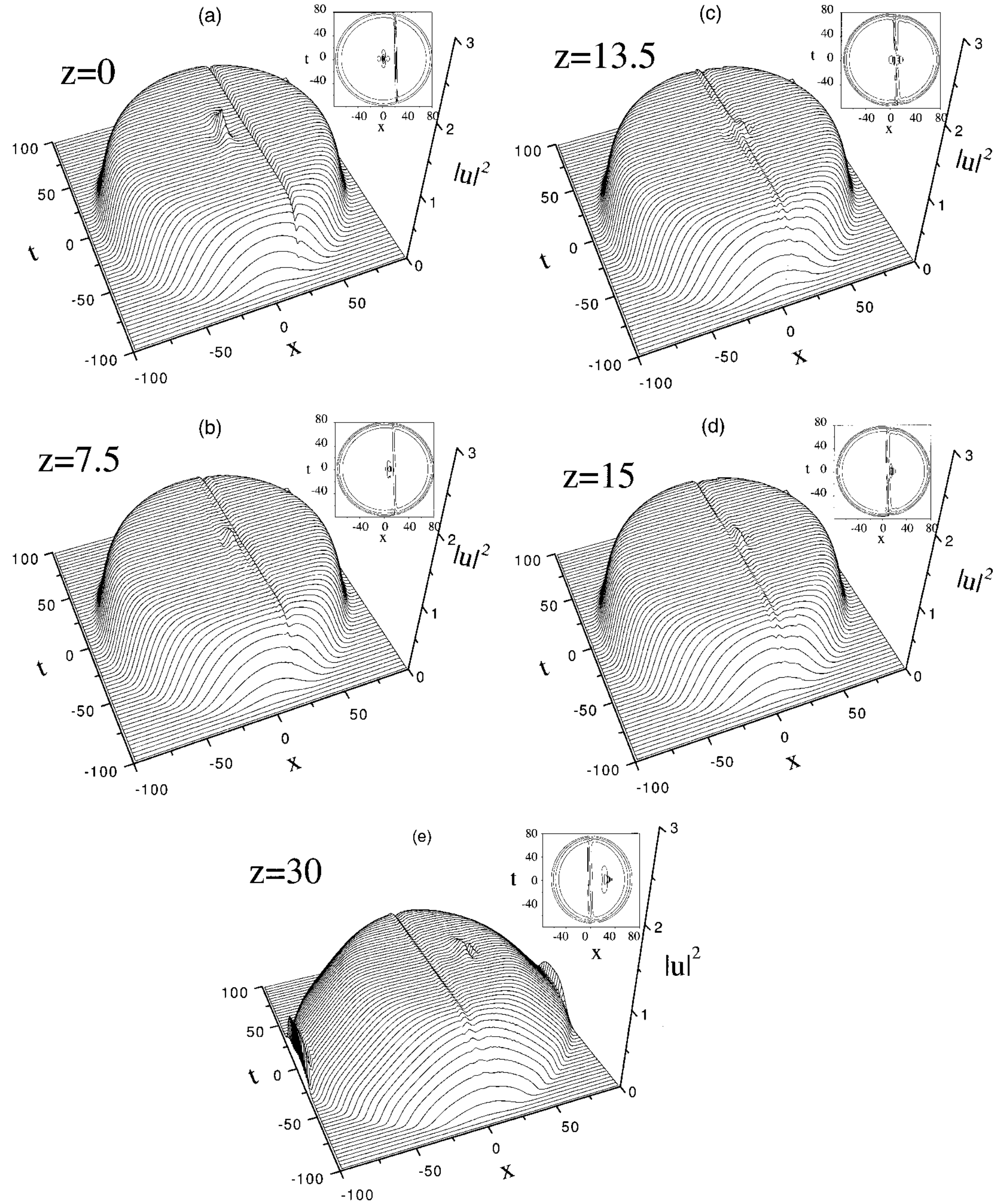

FIG. 1. Evolution of the colliding quasi-one-dimensional dark stripe (with $\kappa_1=1.6$, $\kappa_2=0.2$) and two-dimensional antidark lump (with $\lambda_1=0.8$, $\lambda_2=0.9$) on top of a super-Gaussian cylindrical background. Snapshots of the field are displayed at the values of the propagation distance $z=0$ (a), $z=7.5$ (b), $z=13.5$ (c), $z=15$ (d), and $z=30$ (e). As it is seen, the solitons undergo a quasielastic collision, which is accompanied by a slight deformation of their shapes and emission of a small amount of radiation.

φ_2 to the solitons' amplitudes and phases come into play). Also, notice that a deformation of the super-Gaussian background is observed in Fig. 1(e), which is a precursor of the modulation instability (the latter manifests itself at essentially longer propagation distances, starting from $z\approx 42$).

The final step in our approach is to find postcollision shifts of the soliton trajectories in an analytical form; as was explained in the Introduction, these results are importuned as they make it possible to predict how positions of the lumps may be controlled by passing stripe dark solitons through them. At first, substituting Eqs. (21) and (19) into Eqs. (16) and (17), respectively, we evaluate the solitons' coordinate perturbations ξ_1 and η_1. Then, the solitons' position shifts induced by the headon collision can be obtained as follows. We assume that the solitons A and B, which are described, respectively, by the waveforms $f_1(\xi,X,Z)$ and $g_1(\eta,X,Z)$, are initially far enough from each other, i.e., the soliton A is placed at $\eta=0$ and $\xi=+\infty$, and B is placed at $\xi=0$ and $\eta=-\infty$. Then, long enough after their collision, the shifts Δ_A and Δ_B of the positions of the solitons A and B can be defined as follows: $\Delta_B=\varepsilon[\eta_1(\xi\rightarrow-\infty,X,Z)-\eta_1(\xi\rightarrow+\infty,X,Z)]$ and $\Delta_A=\varepsilon[\xi_1(\eta\rightarrow+\infty,X,Z)-\xi_1(\eta\rightarrow$

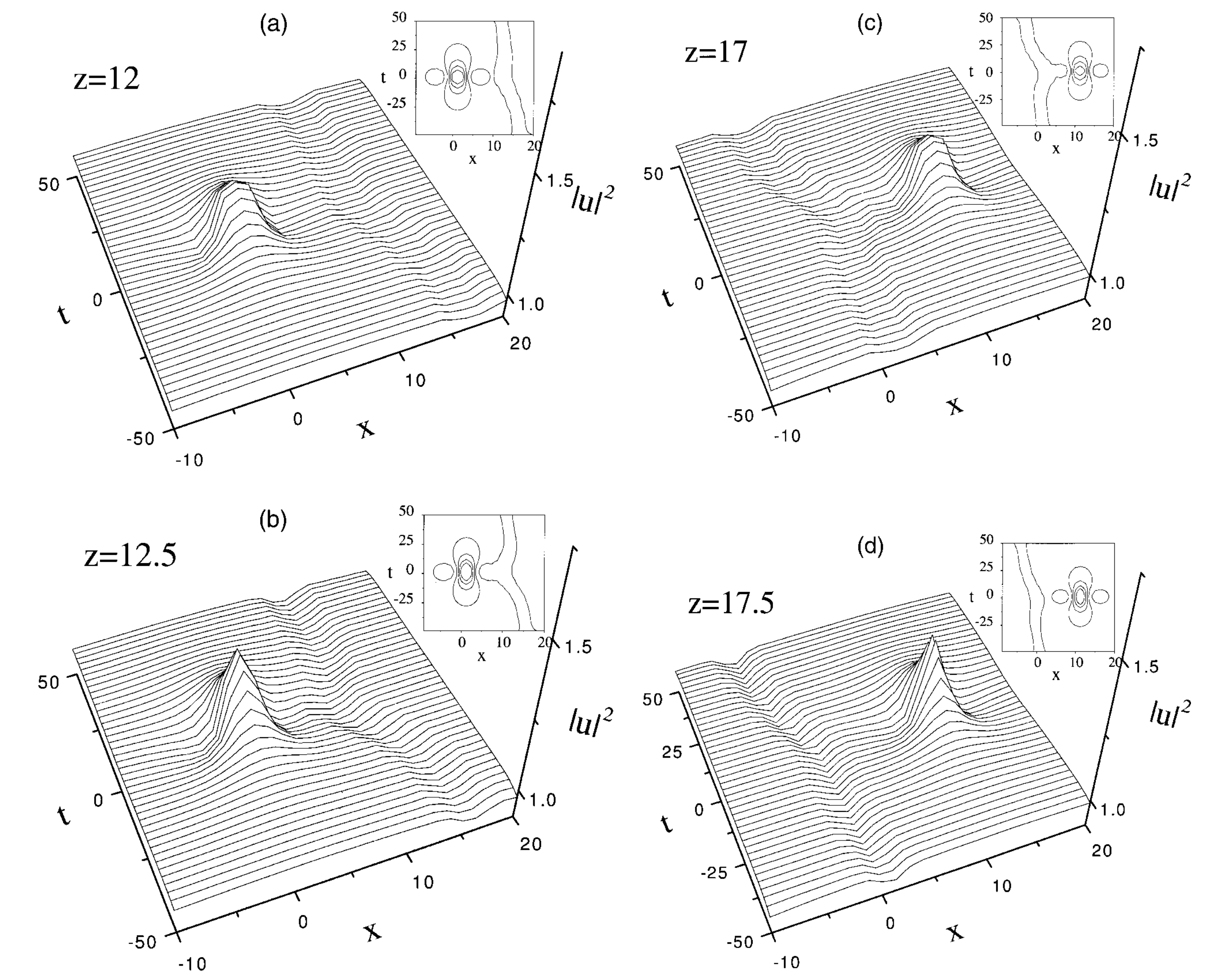

FIG. 2. Details of the evolution of the dark stripe and antidark lump just before their collision, i.e., at $z=12$ (a) and $z=12.5$ (b), and just after the collision, i.e., at $z=17$ (c) and $z=17.5$ (d). As is clearly seen, the dark stripe gets bent and temporarily stuck to the antidark lump due to attraction between them. After the collision, the solitons restore their shape.

$-\infty,X,Z)$]. Nevertheless, in applications, the phase shifts should be obtained for a finite propagation length L; in this case, we may calculate the phase shifts as

$$\Delta_A=\varepsilon[\xi_1(\eta\to L/2)-\xi_1(\eta\to -L/2)]$$

and

$$\Delta_B=\varepsilon[\eta_1(\xi\to -L/2)-\eta_1(\xi\to +L/2)].$$

Following this way, we find that the shift of the 1D dark Q1D stripe soliton is

$$\Delta_A=\varepsilon\,\frac{2\alpha(\delta-8)(\delta+6)}{L|u_0|^2\delta(\delta-2)}. \qquad (25)$$

Note that, in the limit $L\to+\infty$, this phase shift vanishes, which is quite natural, as, in the infinite system, the position of the stripe which has infinite energy cannot be shifted by the interaction with the finite-energy lump. The position shift Δ_B of the 2D elevation lump soliton is

$$\Delta_B=\varepsilon\,\frac{\alpha\kappa_1(\delta-6)(\delta+8)}{2|u_0|^2\delta(\delta+2)}\tanh\left(\frac{\kappa_1 L}{2}\right). \qquad (26)$$

Using the aforementioned values of the physical parameters pertaining to the solitons shown in Figs. 1(a)–1(e), we find that the theoretical predictions given by Eqs. (25) and (26) for the position shifts of the solitons are (for $L=4.5$)

$$\Delta_A=-0.51 \quad \text{and} \quad \Delta_B=-6.9\times 10^{-2}, \qquad (27)$$

for the Q1D dark soliton and 2D elevation lump, respectively.

Since the position shifts are negative, the solitons attract each other, which is also obvious in Fig. 2 that displays details of the collision at the crucial stage when the solitons are interacting strongly. In particular, when the solitons are approaching each other, the dark stripe bends due to the attractive force as is seen in Fig. 2(a) (corresponding to $z=12$) and then it sticks to the lump, see Fig. 2(b), which corresponds to $z=12.5$. Just after the collision (the central point of the collision is $z=15$), the dark stripe is still stuck to the lump as is seen in Fig. 2(c) at $z=17$. Finally, the stripe separates from the lump and moves away, still being bent, as is shown in Fig. 2(d) for $z=17.5$. Notice that for larger values of z (i.e., long enough after the collision), the dark stripe restores its straight-line shape, see Fig. 1(e).

The collision-induced position shifts of the solitons, analytical predictions for which are given by Eq. (27), can be extracted from simulations by means of the following procedure. At first, the simulations are run separately for the quasi-1D dark stripe (soliton A) and 2D lump (soliton B), which are moving to the left and to the right, respectively, along the x axis in the (x,t) plane [see insets in Figs. 1(a)–1(e)]. Thus, assuming that at $z=0$, centers of the solitons A and B were placed at points x_A and x_B, we find the propagation distances, say z_A and z_B, needed for the dark stripe and elevation lump to reach the points x_B and x_A (i.e., for the solitons to interchange their positions). Finally, carrying out the simulations of the actual collision, we find that the soliton A reaches the point x_B and the soliton B reaches the point x_A after passing distances, say z'_A and z'_B, which are different from z_A and z_B because the collision took place. Then, the numerically found position shifts of the solitons are $\hat{\Delta}_A = z_A - z'_A$ and $\hat{\Delta}_B = z_B - z'_B$.

This way, we have found that the numerical position shifts for the solitons, the collision between which is displayed in Figs. 1(a)–1(e), are $\hat{\Delta}_A = -5.95\times 10^{-1}$ and $\hat{\Delta}_B = -8.2\times 10^{-2}$, which appears to be a typical example, if compared to many other runs of the collision simulations not shown here. If these values are compared to the theoretical predictions (27), discrepancies are $\approx 18\%$ for the Q1D dark stripe (soliton A) and $\approx 19\%$ for the elevation lump (soliton B). Having in mind that Eqs. (25) and (26) produce the shifts in the asymptotic approximation, which assumes that the solitons have small amplitudes and, as a matter of fact, they collide at a large relative velocity, we conclude that the agreement between the analytical prediction and direct numerical results is quite reasonable.

IV. CONCLUSIONS

In this work, we used an analytical approach to show that a $(2+1)$-dimensional NLS equation, which includes both the positive second-order and third-order temporal dispersions, supports coexisting soliton solutions of different dimensionality and polarity, propagating on top of a cw background. We have shown that each soliton, viz, a quasi-1D dark stripe and 2D spatiotemporal soliton in the form of an elevated "lump," is governed by its own KP equation and they move in opposite directions. A noteworthy peculiarity of the lump spatiotemporal soliton is that it is weakly (nonexponentially) localized. We have developed a perturbation theory, which shows that, up to the second-order approximation, collisions between these two solitons are elastic. The analytical predictions have been verified by direct numerical integration of the underlying NLS model, with a conclusion that the solitons (especially the quasi-1D dark stripe) indeed restore their shapes after passing through each other. Slight deformation and emission of radiation were also observed, in accord with the analytical approach, which predicts that there exist higher-order corrections to the soliton fields. Additionally, we have analytically calculated position shifts of the solitons induced by the collision that were found to be in quite a reasonable agreement with the numerical results. Using the shifts suggests a natural way to control the position of the lumps in the experiment by passing through them dark stripe solitons launched in the appropriate direction(s).

There exists a possibility of a real experiment to verify theoretical results reported in this work. This can be done using an ordinary planar glass waveguide as a host medium and a broad optical beam, on top of which the solitons are to be created. The necessary strong temporal dispersion can be created by means of a grating. The grating will inevitably induce strong higher-order dispersion, which our model takes into regard.

In fact, the results may have a broader significance, not confined to the field of nonlinear optics, as they provide insight into general aspects of dynamics of multidimensional solitons in nonintegrable systems.

ACKNOWLEDGMENTS

This work has been supported in part by the Special Research Account of the University of Athens (Grant No. 70/4/4095). B.A.M. appreciates the hospitality of the Department of Physics at the University of Athens and support from the Binational (U.S.-Israel) Science Foundation, Grant No. 1999459. Valuable discussions with Dr. Andreas Tsigopoulos (Hellenic Naval Academy) concerning numerical simulations are appreciated.

[1] Y. Silberberg, Opt. Lett. **15**, 1282 (1990).
[2] R. H. Enns, D. E. Edmundson, S. S. Rangnekar, and A. E. Kaplan, Opt. Quantum Electron. **24**, S1295 (1992); D. E. Edmundson and R. H. Enns, Phys. Rev. A **51**, 2491 (1995); D. E. Edmundson, Phys. Rev. E **55**, 7636 (1997).
[3] K. Hayata and M. Koshiba, Phys. Rev. Lett. **71**, 3275 (1993).
[4] B. A. Malomed, P. Drummond, H. He, A. Berntson, D. Anderson, and M. Lisak, Phys. Rev. E **56**, 4725 (1997).
[5] D. V. Skryabin and W. J. Firth, Opt. Commun. **148**, 79 (1998); D. Michalache, D. Mazilu, B. A. Malomed, and L. Torner, *ibid.* **152**, 265 (1998).
[6] H. He and P. Drummond, Phys. Rev. E **58**, 5025 (1998).
[7] X. Liu, L. J. Qian, and F. W. Wise, Phys. Rev. Lett. **82**, 4631 (1999); X. Liu, K. Beckwitt, and F. Wise, Phys. Rev. E **62**,

1328 (2000).

[8] M. Blaauboer, B. A. Malomed, and G. Kurizki, Phys. Rev. Lett. **84**, 1906 (2000).

[9] M. Blaauboer, G. Kurizki, and B. A. Malomed, Phys. Rev. E **62**, R57 (2000).

[10] G. Gottwald, R. Grimshaw, and B. A. Malomed, Phys. Lett. A **248**, 208 (1998).

[11] D. J. Frantzeskakis, K. Hizanidis, B. A. Malomed, and C. Polymilis, Phys. Lett. A **248**, 203 (1998).

[12] P. Di Trapani, D. Caironi, G. Valiulis, A. Dubielis, R. Dalielius, and A. Piskarskas, Phys. Rev. Lett. **81**, 570 (1998).

[13] J. S. Aitchison, A. M. Weiner, Y. Silberberg, M. K. Oliver, J. L. Jackel, D. E. Leaird, E. M. Vogel, and P. W. E. Smith, Opt. Lett. **15**, 471 (1990).

[14] G. P. Agrawal, *Nonlinear Fiber Optics* (Academic, New York, 1995).

[15] M. J. Erro, M. A. G. Laso, D. Benito, E. M. J. Gard, and M. A. Muriel, Fiber Integr. Opt. **19**, 367 (2000).

[16] E. DelRe, S. Trillo, and A. J. Agranat, Opt. Lett. **25**, 560 (2000).

[17] Yu. S. Kivshar, A. Nepomnyashchy, V. Tikhonenko, J. Christou, and B. Luther-Davies, Opt. Lett. **25**, 123 (2000).

[18] V. I. Petviashvili and O. A. Pokhotelov, *Solitary Waves in Plasmas and in the Atmosphere* (Gordon and Breach, New York, 1992).

[19] A. Jeffrey and T. Kawahara, *Asymptotic Methods in Nonlinear Wave Theory* (Pitman, London, 1982).

[20] P. Di Trapani, W. Chinaglia, S. Minardi, A. Piskarskas, and G. Valiulis, Phys. Rev. Lett. **84**, 3843 (2000).